ChemComm
Chemical Communications

Accepted Manuscript

This article can be cited before page numbers have been issued, to do this please use: E. Mathieu, A. Bernard, E. Quévrain, M. Zoumpoulaki, S. Iriart, C. Lung-Soong, B. Lai, K. Medjoubi, L. Henry, S. Nagarajan, F. Poyer, A. Scheitler, I. Ivanovic-Burmazovic, S. Marco, A. somogyi, P. Seksik, N. Delsuc and C. Policar, *Chem. Commun.*, 2020, DOI: 10.1039/D0CC03398G.

ROYAL SOCIETY OF CHEMISTRY

rsc.li/chemcomm

View Article Online
DOI: 10.1039/D0CC03398G

COMMUNICATION

Intracellular location matters: rationalization of the anti-inflammatory activity of a manganese (II) superoxide dismutase mimic complex

Received 00th January 20xx,
Accepted 00th January 20xx

DOI: 10.1039/x0xx00000x

Emilie Mathieu,[a] Anne-Sophie Bernard,[a] Elodie Quévrain,[a] Martha Zoumpoulaki,[a] Sébastien Iriart,[a] Caroline Lung-Soong,[a] Barry Lai,[b] Kadda Medjoubi,[c] Lucas Henry,[a] Sounderya Nagarajan,[d,e] Florent Poyer,[d,e] Andreas Scheitler,[f] Ivana Ivanović-Burmazović,[f] Sergio Marco,[d,e] Andrea Somogyi,[c] Philippe Seksik,[g] Nicolas Delsuc,[a] and Clotilde Policar*[a]

A conjugate of a Mn-based superoxide dismutase mimic with a Re-based multimodal probe 1 was studied in a cellular model of oxidative stress. Its speciation was investigated using Re and Mn X-fluorescence. Interestingly, 1 shows a distribution different from its unconjugated analogue but a similar concentration in mitochondria and a similar bioactivity.

A new class of metallo-drugs with catalytic activity and inspired from metalloenzymes are emerging: they are of interest as they may allow decreasing the administered doses thus reducing potential side effects, toxicity and treatment costs.[1-3] Superoxide dismutase mimics, SOD mimics,[4-13] belong to this family of catalytic drugs. They reproduce the catalytic activity of superoxide dismutases, metalloproteins involving Cu-Zn, Mn, Fe, Ni or Cu at the active site that protect the cell against oxidative stress by catalysis of superoxide dismutation.[14, 15]

Their use in a biological context raises new challenges. Indeed, parameters other than intrinsic catalytic activity are essential for good efficacy: cell penetration, speciation, and intracellular location(s) and concentration(s).[16] It is therefore important to investigate the activity of SOD mimics directly in the cellular environment under oxidative stress, which is defined as an imbalance between the production of reactive oxygen species (ROS) and endogenous antioxidants.[17, 18] Some pathologies, such as inflammatory bowel diseases (IBD) or amyotrophic lateral sclerosis (ALS), have been associated with impairment of SOD, either because the enzyme is under-expressed or expressed in an inactive form.[19, 20] SOD mimics are able to substitute for SODs in SOD-deficient organisms, protect against radiation and ischemia-reperfusion injuries, and limit inflammation and other pathological processes associated with oxidative stress.[5-8, 11, 21] Most of the metal complexes studied in the literature for their bioactivity are used as anticancer or antibacterial agents, thus most bioanalyses focus on their toxicity towards cancer cells or micro-organisms. In contrast, SOD-mimics are meant to restore normal functioning of cells by limiting oxidative stress. As such, specific non-routine strategies are required to evaluate their bioactivity.[4, 22, 23] We have recently set up several cellular models of oxidative stress,[4, 22-24] one of which consists of epithelial cells in which inflammation can be induced,[25, 26] which can be used to probe the bioactivity of SOD mimics.[22] A key question for rationalizing the bioactivity of a molecule is its intracellular concentration. The actual quantity in cells, and not the concentration of incubation, is an important consideration for rationalizing the activity.[2, 22, 27] In addition, cells are compartmented, so bioactivity depends on the sub-cellular distribution. In the case of protection against oxidative stress, mitochondria are believed to be a fragile site that requires specific protection.[28, 29]

In the present work, we have designed a new Mn-SOD mimic **1** (Fig. 1) that was obtained by conjugation of a Re-tris carbonyl probe that can be used for several imaging modalities,[30-33] including X-Ray fluorescence,[31] to the parent Mn-SOD mimic **2**. This enabled us to image Mn and Re directly, in order to correlate distribution of Mn with that of the Re-tagged ligand, providing an insight into the stability of the SOD mimic in cells. We have studied the bioavailability and intracellular distribution of **1**. Its activity in cells was determined and compared with the non-conjugated parent complex **2**. Surprisingly, the new conjugate **1** showed a markedly different intracellular distribution and accumulation, while displaying overall similar bioactivity to the unconjugated analogue **2**. Interestingly, the concentration of **1** and **2** are similar at the mitochondria, which is recognized to be the fragile organelle to be protected under oxidative stress.

[a] Laboratoire des biomolécules, LBM, Département de chimie, Ecole normale supérieure, PSL University, Sorbonne université, CNRS, 75005 Paris, France. E-mail: clotilde.policar@ens.fr
[b] X-ray Science Division, Argonne National Laboratory, Argonne, Illinois 60439, United States.
[c] Synchrotron SOLEIL, BP 48, Saint-Aubin, 91192 Gif sur Yvette, France
[d] Institut Curie, Research Center, PSL University, Chemistry, Modelling and Imaging for Biology (CMIB), Bât 110-112, Centre Universitaire, F-910405 Orsay, France
[e] INSERM U 1196, CNRS UMR 9187, Paris-Saclay University, Paris-Sud University, University Centre, Orsay, France
[f] Department of Chemistry and Pharmacy, University of Erlangen-Nürnberg, Egerlandstr. 1, 91058 Erlangen, Germany
[g] Sorbonne Université, Ecole normale supérieure, PSL University, CNRS, INSERM, AP-HP, Laboratoire des biomolécules, LBM 75012 Paris, France
†Electronic Supplementary Information (ESI) available: experimental procedures, supplementary figures and tables. See DOI: 10.1039/x0xx00000x

This study is in line with other works meant to better understand the bioactivity of SOD mimics, including works on mechanisms of SOD mimics,[34-36] on the application of SOD mimics,[7, 10, 13, 37, 38] or on the distribution and speciation of these compounds.[16, 22, 39, 40]

The multimodal probe was synthesized with a pendant aldehyde moiety meant for conjugation with the ligand **L2** via a reductive amination coupling (ESI §5). The effect of functionalization on the lipophilicity of the **L2** ligand was studied using analytical HPLC (ESI §6), showing that coupling with the probe increased the retention time of **L1** compared to **L2** on the reversed-phase C18 column, and thus the lipophilicity of the molecule (Fig. S5).[41] The conjugation did not modify the fluorescence nor the IR properties of the probe (Fig. S1 and S2). **L1** was purified by HPLC and titrated by UV-visible spectrophotometry (ESI §6-7). Metalation with $MnCl_2$ leads to the formation of **1** (ESI for characterization §7).

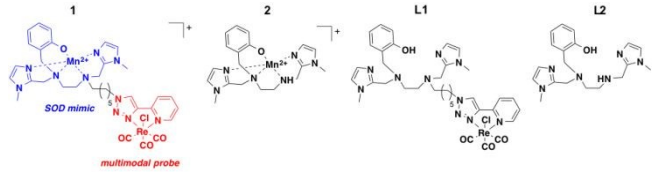

Figure 1. Structures of **1**, **2**, **L1**, and **L2**.

Cyclic voltammetry experiments at different scan rates were performed in HEPES buffer (0.1 M, pH 7.5) (Fig. S3). A quasi-reversible system was obtained with ΔE_p = 90 mV at 50 mV/s. The apparent standard potential of **1** is of 243 mV *vs*. SCE (saturated calomel electrode), slightly higher than for **2** (196 mV *vs.* SCE).[42] A similar difference in potential has been previously described for similar functionalization of **L1**,[43] and other complexes containing amine based-ligands,[44, 45] associated with the weaker basicity of a tertiary amine. Importantly, this value remains in the range appropriate for superoxide dismutation.[4] The dissociation constants (K_d) were determined spectrophotometrically to be 9 ± 4 10^{-8} and 7 ± 3 10^{-7} at pH7.5 for **1** and **2** respectively (see Fig. S4 and ESI §7), which is similar to previous measurements for **2**.[22, 43, 46] These association constants mean that in the incubation conditions (100 µM), 97% of **L1** and 92% of **L2** are coordinated.

The intrinsic SOD activity, or activity outside of any cellular context, was determined by the McCord-Fridovich assay (Table S1) and provided as a k_{McCF} (ESI §3). The k_{McCF} of **1** is 6.4 x 10^6 $M^{-1}.s^{-1}$, similar to the constant previously reported for **2** (7.0 x 10^6 $M^{-1}.s^{-1}$).[42] The SOD-like activity of **1** was also investigated with a high excess of superoxide using a direct stopped-flow measurement combined with fast diode-array UV-vis detection.[36, 43, 47] The k_{cat} value was 6.46 x 10^6 $M^{-1}.s^{-1}$ in MOPS buffer (60 mM, ionic strength 150 mM, pH 7.8) is consistent with the k_{McCF}, confirming that coupling with the probe does not change the intrinsic SOD activity of the SOD mimic.

The bioactivity was investigated in a cellular model of oxidative stress. Briefly, in this model, human intestinal epithelial cells HT29-MD2 are activated with bacterial lipopolysaccharide (LPS), a component of bacteria cell-membrane, to generate an inflammatory reaction associated with oxidative stress in cells.[22, 25, 26] Prior to the study of the cellular bioactivity of the complex, we characterized the bioavailability of the complexes in HT29-MD2, by studying the accumulation and subcellular location of **1**. The quantification of the total manganese content was determined by electron paramagnetic resonance (EPR) titration in HT29-MD2 cells after a 6-hour incubation with **1** and acid treatment to release Mn from all coordination sites.[22] We also compared the Mn-content in a fraction enriched in mitochondria using inductively coupled plasma mass spectrometry (ICP-MS), which provides a higher sensitivity than EPR (ESI, §8). The quantification indicates that intracellular overall accumulation is higher for **1** than for **2**, (Fig. 2A.a., C vs. B) whereas the Mn-content in the mitochondrial fraction was not significantly different for cells incubated with **1** or **2** (Fig. 2A.b., C vs. B).

Cells incubated with **1** were studied by IR and X-ray fluorescence microspectroscopies. To avoid possible re-localization upon chemical fixation and drying, we have used a cryofixation-lyophilisation procedure, as previously described.[22] Fourier transform infrared spectromicroscopy (FTIR-SM) showed the two IR-bands (A1 and E) of the Re-tris-carbonyl core in cryofixed and freeze-dried HT29-MD2 cells incubated with **1** (ESI §8 and Fig. S9).

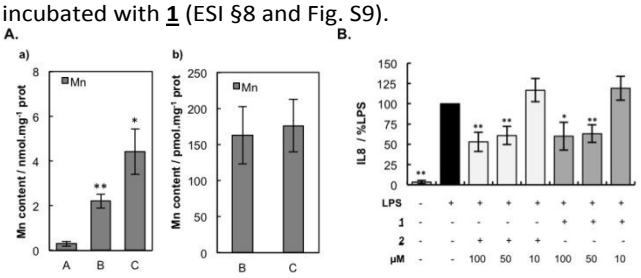

Figure 2. A. Quantification of total Mn content in cell lysates (a), or mitochondria-enriched fractions (b). HT29-MD2 cells were incubated for 6 hours under different conditions: A: medium only; B: **2** (100 µM); C: **1** (100 µM, 0.02%DMSO). a: Total Mn content was determined in acid-digested cell lysates by titration using EPR (ESI). Data represent mean ± SEM for 4 independent experiments. (*) $p < 0.05$, (**) $p < 0.01$ vs. A. b: Total Mn content was determined in mitochondria-enriched fractions by ICP-MS. Mitochondria were isolated using a mitochondria isolation kit (Thermo Fisher Scientific). Data represent mean ± SEM for 7 independent experiments.

B. IL8 secretion in HT29-MD2 cells. Intestinal epithelial cells HT29-MD2 were incubated for 7 hours under different conditions indicated in the figure. LPS (0.1 µg.mL^{-1}) was added at the end of the first hour. Data represent means ± SEM for 7-10 independent experiments. (*) $p < 0.05$, (**) $p < 0.01$ vs. B.

The intracellular distribution of **1** was further studied by SR-XRF. With this technique, heavy elements can be mapped in a single cell with good spatial resolution (ca. 300 nm).[48-50] Figure 3 shows the distribution of phosphorus (P), manganese (Mn), zinc (Zn) and rhenium (Re) in a single cryofixed HT29-MD2 cell. The mapping of P and Zn (K-lines) reveals the nucleus location.[51] Since Re is an ultratrace element in biological samples,[52] the Re signal observed (L-lines, see ESI) can be assigned to the presence of the ligand **L1** or of the complex. Note that the Mn map corresponds to that of **1** and endogenous Mn, the latter being less abundant (see Fig. 2A). As can be seen from the overlay of Mn and Re maps, part of the Mn map overlaps with that of the Re, suggesting that in these areas (white Fig. 2B, Fig. S14 and Fig. S15) complex **1** can

still be intact. Moreover, it shows that **1** is not homogeneously distributed, but has a perinuclear distribution with a punctate appearance. This is a striking difference from the homogenous distribution of **2** in cells and from the distribution of Mn in cells incubated with $MnCl_2$.[22] In addition, cells were co-incubated with a mitochondrial marker, Mitotracker™ deep red, before cryofixation and freeze-drying, and fluorescence images of stained cells were recorded before X-fluorescence analysis (Fig.S12 and S13). Overlay of the Mitotracker signal with the Re map (Fig. S13) showed areas where the two signals overlap. This revealed that **1** is localized in perinuclear organelles including mitochondria, but not exclusively: **1** was clearly also localized in organelles other than mitochondria. The more hydrophobic nature of **L1** could explain the accumulation of **1** in membrane-rich organelles.

Finally, X-fluorescence spectroscopy can provide quantitative information on the amount of heavy elements in cells. Using the appropriate standards, we were able to determine the amount of Mn and other elements (P, S, K, Fe) in cells (Fig. S11). The average concentration of Mn for cells incubated with **1** is 6.8 ± 0.7 ng/cm^2, which is in the same range as other Mn-complexes (5 to 60 ng/cm^2) described in literature.[39, 40]

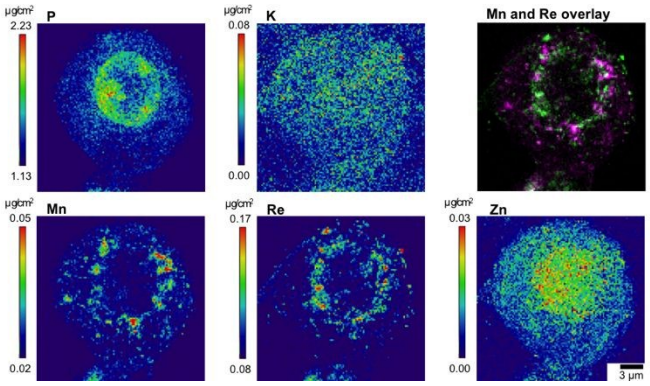

Figure 3. Elemental distribution of P, K, Mn, Re, and Zn in a HT29-MD2 cell incubated with **1**. The phosphorus (P), and zinc (Zn, K-lines) maps are used to identify the nucleus area. The overlay (top right) corresponds to the Mn (magenta) and Re (L-lines) (green) maps. The regions corresponding to an overlap of both elements are displayed in white. Intestinal epithelial cells HT29-MD2 were incubated for 2 hours with **1** (100 µM, 0.02%DMSO) before cryofixation and freeze-drying. Images were recorded on the 2-ID-D beamline of APS synchrotron (excitation at 12.0 keV; integration time, 2 s/pixel; pixel size, 200 nm). Scale bar, 3 µm.

The anti-inflammatory activity of **1** was investigated in HT29-MD2 activated by LPS, used as a cellular model of oxidative stress.[22] Two markers of inflammation, interleukin 8 (IL8) secretion (Fig. 2B, and S7) and cyclooxygenase 2 (COX2) expression (Fig. S8), were evaluated. These two markers are overexpressed in LPS-activated HT29-MD2 cells, which is consistent with the generation of an inflammatory reaction.[22] **1** and **2** were assayed at 100, 50, and 10 µM incubation concentrations at which no toxicity was observed, with or without LPS (Fig. S6). Interestingly, both compounds exert a similar anti-inflammatory activity in LPS-activated cells at 100 and 50 µM as can be seen from the decrease in IL8 secretion (Fig. 2B) and COX2 expression (Fig. S8) compared to LPS-activated cells. No effect of the compounds was observed at 10 µM. They both had a weak pro-inflammatory effect when used on non-activated cells at 100 or 50 µM (Fig. S7). The Zn^{II} complexes were used as redox inactive analogues of **2** [22] and **1** and displayed no effect on IL8 production on LPS-activated, or non-activated cells (Fig. S7). Note that DMSO, which is used to solubilize **1** and was present in the cell culture medium at a final concentration of 0.02% (v/v), showed no effect on IL8 production (Fig. S7). Finally, $MnCl_2$ also does not exhibit any anti-inflammatory activity (Fig. S7) Altogether these data demonstrate that **1** has an anti-inflammatory activity similar to **2** in LPS-activated cells. This anti-inflammatory activity is associated with their redox properties, as the zinc-analogues have shown no effect (Fig. S7).

The mitochondrial manganese SOD (MnSOD) is overexpressed in cells activated with LPS (Fig. S8) as a feedback response of the cell against oxidative stress.[22, 53-55] **1** efficiently decreases MnSOD overexpression at 100 and 50 µM in LPS activated cells, with no detectable effect at 10 µM, which correlates well with the IL8 and COX2 data (Fig. S7-S8). Its ability to limit MnSOD overexpression in LPS-activated cells can be interpreted as an efficient anti-superoxide effect.[22] Interestingly, like **2**, **1** is able to complement SOD and to protect mitochondria from oxidative damage. The conjugation to the Re-tris carbonyl probe did not change the overall biological activity of the complex, although it changed drastically its location.

Anti-inflammatory and antioxidant effects of **2** and **1** are in a similar range, as demonstrated by IL8, COX2, and MnSOD expression levels: both complexes are efficient in cells and can reach their target(s). In addition, **2** and **1** are able to complement the mitochondrial MnSOD under stress conditions. Surprisingly, **1** and **2** have a similar bioactivity, while showing a different overall concentration and a marked different cellular distribution, but a similar mitochondrial Mn-content. Finally, this similar mitochondrial Mn-content bioactivity associated with a similar bio-activity makes sense as mitochondria are believed to require specific protection under oxidative stress.[28, 29] This stresses the fact that bioactivities are compartmentalized: “more in cells” does not track with “better bioactivity”. We propose that context-dependent bioactivity is a key factor for the efficacy of these new classes of metallodrugs. More generally, to rationalize bioactivities, correlations are required, not with the incubation concentration or overall intracellular location, but ideally with the concentration at a specific location.

Conflicts of interest

Philippe Seksik declares consulting fees from Takeda, Abbvie, Merck-MSD and Biocodex, grants from Biocodex, sponsored travel from Merck-MSD and Takeda. These COI are not related with the present work.

Acknowledgements

We thank Ecole Normale Supérieure Paris Saclay for E. Mathieu’s PhD fellowship, TGE RENARD (FR 3443, CNRS) and UMR8601 and S. Lajnef for access to the EPR spectrometer for the EPR experiments,

View Article Online
DOI: 10.1039/D0CC03598G

Dr. J.L. Guerquin-Kern, Dr. S. Trepout and Dr. T.-D. Wu, for useful discussions and help in cryofixed samples sample preparation, Dr. F. Lambert for help in synthesis, Z. Gueroui for access and help with the fluorescence microscope at ENS and S. Clède for help in the recording of fluorescence images, B. Goetz for help with ICP-MS, Pr. A. Leturque and M. Moreau for access to the WES, Dr. G. Sommeria-Klein and Dr. A. Tebo for useful discussions. Association François Aupetit, ANR (ANR-10-IDEX-0001-02 PSL* project INOCELLCHEM and ANR-15-CE07-0027 project MAGIC), Fondation pour la Recherche Biomédicale (project DIE20151234413) are acknowledged for financial supports; SOLEIL and APS committees for beamtime. Use of the Advanced Photon Source, an Office of Science User Facility operated for the U.S. Department of Energy (DOE) Office of Science by Argonne National Laboratory, was supported by the U.S. DOE under Contract No. DE-AC02-06CH11357.

Notes and references

1. A. L. Noffke, A. Habtemariam, A. M. Pizarro and P. J. Sadler, *Chem. Commun.*, 2012, **48**, 5219-5246.
2. J. Suh and W. S. Chei, *Curr. Op. Chem. Biol.*, 2008, **12**, 207-213.
3. J. J. Soldevila-Barreda and P. J. Sadler, *Curr. Op. Biol. Chem.*, 2015, **25**, 172-183.
4. C. Policar, in *Redox Active Therapeutics*, eds. J. S. Reboucas, I. Batinic-Haberle, I. Spasojevic, D. S. Warner and D. St. Clair, Springer, 2016, ch. Chapter 17, pp. 125-164.
5. S. Miriyala, I. Spasojevic, A. Tovmasyan, D. Salvemini, Z. Vujaskovic, D. St. Clair and I. Batinic-Haberle, *Biochim. Biophys. Acta*, 2012, 794-814.
6. C. Muscoli, S. Cuzzocrea, D. P. Riley, J. L. Zweier, C. Thiemermann, Z.-Q. Wang and D. Salvemini, *Br. J. Pharmacology*, 2003, **140**, 445-460.
7. D. Salvemini, C. Muscoli, D. P. Riley and S. Cuzzocrea, *Pulm. Pharmacol. Ther.*, 2002, **15**, 439-447.
8. I. Batinic-Haberle, A. Tovmasyan, E. R. Roberts, Z. Vujaskovic, K. W. Leong and I. Spasojevic, *Antiox Redox Signal.*, 2014, **20**, 2372-2415.
9. I. Batinić-Haberle, J. S. Rebouças and I. Spasojević, *Antiox Redox Signal.*, 2010, **13**, 877-918.
10. O. Iranzo, *Bioorg. Chem.*, 2011, **39**, 73-87.
11. A. Haber and Z. Gross, *Chem. Commun.*, 2015, **51**, 5812-5827.
12. D. Salvemini, Z.-Q. Wang, J. L. Zweier, A. Samouilov, H. Macarthur, T. P. Misko, M. G. Currie, S. Cuzzocrea, J. A. Sikorski and D. P. Riley, *Science*, 1999, **286**, 304-305.
13. R. Bonetta, *Chem. Eur. J.*, 2018, **24**, 5032-5041.
14. Y. Sheng, I. A. Abreu, D. E. Cabelli, M. J. Maroney, A.-F. Miller, M. Teixeira and J. S. Valentine, *Chem. Rev.*, 2014, **114**, 3854-3918.
15. J. E. Gleason, A. Galaleldeen, R. L. Peterson, A. B. Taylor, S. P. Holloway, J. Waninger-Saroni, B. P. Cormack, D. E. Cabelli, P. J. Hart and V. C. Culotta, *Proc. Natl. Acad. Sci. U.S.A.*, 2014, **111**, 5866-5871.
16. R. L. McNaughton, A. R. Reddi, M. H. S. Clement, A. Sharma, K. Barnese, L. Rosenfeld, E. Butler Gralla, J. S. Valentine, V. C. Culotta and B. Hoffman, *Proc. Natl. Acad. Sci. U.S.A.*, 2010, **107**, 15335-15339.
17. M. Schieber and N. S. Chandel, *Curr. Biol.*, 2014, **24**, R453-R462.
18. B. Halliwell and J. M. C. Gutteridge, *Free radicals in biology and medicine* Oxford University Press, New York 2007.
19. A. Ferri, M. Cozzolino, C. Crosio, M. Nencini, A. Casciati, E. B. Gralla, G. Rotilio, J. S. Valentine and M. T. Carri, *Proc. Natl. Acad. Sci. U.S.A.*, 2006, **103**, 13860-13865.
20. L. Kruidenier, I. Kuiper, W. van Duijn, S. L. Marklund, R. A. van Hogezand, C. B. H. W. Lamers and H. W. Verspaget, *J. Pathol.*, 2003, **201**, 7-16.
21. I. Batinic-Haberle and I. Spasojevic, *Antiox Redox Signal.*, 2014, **20**, 2323-2325.
22. E. Mathieu, A.-S. Bernard, N. Delsuc, E. Quévrain, G. Gazzah, B. Lai, F. Chain, P. Langella, M. Bachelet, J. Masliah, P. Seksik and C. Policar, *Inorg. Chem.*, 2017, **56**, 2545-2555.
23. A.-S. Bernard, C. Giroud, H. Y. V. Ching, A. Meunier, V. Ambike, C. Amatore, M. Guille Collignon, F. Lemaître and C. Policar, *Dalton Trans.*, 2012, **41**, 6399-6403.
24. A. Vincent, J. R. Fores, E. Tauziet, E. Quévrain, A. Dancs, A. Conte-Daban, A.-S. Bernard, P. Pelupessy, K. Coulibaly, P. Seksik, C. Hureau, K. Selmeczi, C. Policar and N. Delsuc, *Chem. Commun.*, 2020, **56**, 399-402.
25. C. Lenoir, C. Sapin, A. H. Broquet, A.-M. Jouniaux, S. Bardin, I. Gasnereau, G. Thomas, P. Seksik, G. Trugnan, J. Masliah and M. Bachelet, *Life Sci.*, 2008, **82**, 519-528.
26. P. Seksik, H. Sokol, V. Grondin, C. Adrie, H. Duboc, B. Pigneur, G. Thomas, L. Beaugerie, G. Trugnan, J. Masliah and M. Bachelet, *Innate Imunnity*, 2010, **16**, 381-390.
27. B. A. Gilston and T. O'Halloran, in *Metals in cells*, eds. V. Cullota and R. A. Scott, Wiley, 2013, ch. Introduction.
28. N. Apostolova and V. M. Victor, *Antiox. Redox Sign.*, 2015, **22**, 686-729.
29. R. A. J. Smith, R. C. Hartley and M. P. Murphy, *Antiox. Redox Sign.*, 2011, **15**, 3021-3038.
30. M. P. Coogan and V. Fernández-Moreira, *Chem. Commun.*, 2013, **50**, 384-399.
31. S. Hostachy, C. Policar and N. Delsuc, *Coord. Chem. Rev.*, 2017, **351**, 172-188.
32. S. Clède and C. Policar, *Chem. Eur. J.*, 2015, **21**, 942-958.
33. E. Licandro, M. Panigati, M. Salmain and A. Vessières, in *Bioorganometallics-Biomolecules, labeling, medecine*, ed. G. Jaouen, Wiley-VCH, Weinheim, 2015, vol. 1, pp. 341-391.
34. K. Barnese, E. Butler Gralla, J. S. Valentine and D. E. Cabelli, *Proc. Natl. Acad. Sci. U.S.A.*, 2012, **109**, 6892-6897.
35. K. Barnese, E. B. Gralla, D. E. Cabelli and J. S. Valentine, *J. Am. Chem. Soc.*, 2008, **130**, 4604-4606.
36. I. Kenkel, A. Franke, M. Dürr, A. Zahl, C. Dücker-Benfer, J. Langer, M. R. Filipović, M. Yu, R. Puchta, S. R. Fiedler, M. P. Shores, C. R. Goldsmith and I. Ivanović-Burmazović, *J. Am. Chem. Soc.*, 2017, **139**, 1472-1484.
37. S. Signorella, C. Palopoli and G. Ledesma, *Coord. Chem. Rev.*, 2018, **365**, 75-102.
38. I. Batinic-Haberle, A. Tovmasyan and I. Spasojevic, *Antiox Redox Signal.*, 2018, **29**, 1691-1724.
39. J. B. Aitken, E. L. Shearer, N. M. Giles, B. Lai, S. Vogt, J. S. Reboucas, I. Batinic-Haberle, P. A. Lay and G. I. Giles, *Inorg. Chem.*, 2013, **52**, 4121-4123.
40. C. M. Weekley, I. Kenkel, R. Lippert, S. Wei, D. Lieb, T. Cranwell, J. L. Wedding, A. S. Zillmann, R. Rohr, M. R. Filipovic, I. Ivanović-Burmazović and H. H. Harris, *Inorg. Chem.*, 2017, **56**, 6076-6093.
41. K. Valko, *J. Chromatography A*, 2004, **1037**, 299-310.
42. F. Cisnetti, A. S. Lefevre, R. Guillot, F. Lambert, G. Blain, E. Anxolabéhère-Mallart and C. Policar, *Eur. J. Inorg. Chem.*, 2007, 4472-4480.
43. H. Y. V. Ching, I. Kenkel, N. Delsuc, E. Mathieu, I. Ivanović-Burmazović and C. Policar, *J. Inorg. Biochem.*, 2016, **160**, 172-179.
44. D. Meyerstein, *Coord. Chem. Rev.*, 1999, **185-6**, 141-147.
45. E. K. Barefield, *Coord. Chem. Rev.*, 2010, **254**, 1607-1627.
46. A. Conte-Daban, V. Ambike, R. Guillot, N. Delsuc, C. Policar and C. Hureau, *Chem. Eur. J.*, 2018, **24**, 5095-5099.
47. F. C. Friedel, D. Lieb and I. Ivanovic-Burmazovic, *J. Inorg. Biochem.*, 2012, **109**, 26-32.
48. Q. Jin, T. Paunesku, B. Lai, S.-C. Gleber, S. Chen, L. Finney, D. Vine, S. Vogt, G. Woloschak and C. Jacobsen, *J. Microscopy*, 2017, **265**, 81-93.
49. B. Wu and J. S. Becker, *Int. J. Mass Spec.*, 2011, **307**, 112-122.
50. C. J. Fahrni, *Curr. Op. Chem. Biol.*, 2007, **11**, 121-127.
51. R. McRae, B. Lai and C. J. Fahrni, *Metallomics*, 2012, **5**, 52-61.
52. I. Rodushkin, E. Engström, A. Stenberg and D. C. Baxter, *Anal. Bioanal. Chem.*, 2004, **380**, 247-257.
53. J. F. Valentine and H. S. Nick, *Gastroenterology*, 1992, **103**, 905-912.
54. H. S. Nick, R. J. Rogers and J. M. Monnier, *J. Biol. Chem.*, 2001, **276**, 20419-20427.
55. S. H. H. Chan, K. L. H. Wub, L. L. Wang and J. Y. H. Chan, *Free Radical Biol. Med.*, 2005, **39**, 603-618.